Control of Bilateral Teleoperation Systems

İlhan Polat

Control of Bilateral Teleoperation Systems

Proefschrift

ter verkrijging van de graad van doctor
aan de Technische Universiteit Delft,
op gezag van de Rector Magnificus prof. ir. K.C.A.M. Luyben,
voorzitter van het College voor Promoties,
in het openbaar te verdedigen op donderdag 45 juli 2012 om 23:30 uur
door İlhan Polat,
ingenieur werktuigbouwkunde,
geboren te Gaziantep, TURKIJE.

Dit proefschrift is goedgekeurd door de promotor:
Prof.dr. C.W. Scherer

Samenstelling promotiecommissie:

Rector Magnificus	voorzitter
Prof.dr. C.W. Scherer	Universität Stuttgart, promotor
Prof.ir. Prof. 1	Technische Universiteit Delft
Prof.dr.ir. M. Steinbuch	Technische Universiteit Eindhoven
Prof. Someone2	ETH Zürich
Prof.ir. Whoelse	Technische Universiteit Delft
Dr. Him Too	University of Virginia
Dr.ir. John Doe	NASA

This thesis has been completed in partial fulfillment of the requirements of the Dutch Institute for Systems and Control (DISC). The work was supported under the Microfactory project by MicroNed, a consortium to nurture micro systems technology in The Netherlands.

Published and distributed by: İlhan Polat
E-mail: i.polat@tudelft.nl

ISBN 000-00-0000-000-0

Printed by some company

Contents

List of Tables

List of Figures

CHAPTER 1

Introduction

The success of the technological advances often can be associated with an unprecedented convenience that they bring in. At the heart of this convenience lies the ability to relax the limitations of the human body to a certain extent. From this point of view, it is not a surprise that the three most prominent technological wonders of the last century, namely the *Television*, the *Telephone* and the *radio* (which was originally called “radiotelegraphy"), bears the same Greek prefix *tele-* which corresponds to “*at a distance*" in our context. This shows that there is something of extreme importance about our drive to extend our capabilities beyond the constraints that our bodies impose.

It is quite remarkable, in retrospect, that these “gadgets" did not perish but rather kept on evolving since initially they were far from perfect. Quite the contrary, they were hardly operational. Even the commercialized version of the early TVs had a narrow bandwidth and minimum image quality. Similarly radio and telephone was barely transmitting sensible information as far as the signal-to-noise ratio is concerned. Nevertheless, they have provided the ways of communication which were unimaginable before their time. Therefore the added value dominated the shortcomings and even though they were quite imperfect, we kept using them. The important lesson to be learned was that a technology should not be judged by its imperfections but rather should be weighed by its contribution in this context or the convenience that is brought in by using it.

The success is also related to the fact that these technologies mainly relied on the human brain itself at their early stages. For example, the human brain did most of the noise filtering and data recovery by just guessing the missing pieces and identifying patterns from the signal brought by the respective medium. Today, with our smart mobile phones and 3D LED TVs, we can assume that the computational load on the human brain is drastically reduced. In other words, we are still identifying patterns and utilizing the relevant parts of our brain to make sense out of a TV broadcast[1]. However, we don’t need to use a higher level of concentration to reconstruct the words that we hear or to identify the image on the display due to the high quality output.

It seems that we are on the same track with the technological developments involving our touch sense. Considering the importance of our touch sense in any given situation, the added value of extending of our perception in this modality needs no motivation. Take the most familiar example: the vibrating mobile phone in the silent mode in our pocket. This is a very important example since every individual learns what that vibration might mean, either

[1]Pun intended.

an SMS or a call, depending on the vibrational pattern. This means that the touch sense can be used to convey messages and more importantly we can process those messages for inference.

This type of information said to be received via the haptic channel (or the collaborative use of tactile and proprioceptive modalities). Note that, we use the term "touch sense" pretty vaguely as a shortcut and we leave it to the experts of the field to define the sophisthicated mechanisms (pertaining to the somatosensory system) that we utilize when we manipulate objects, say with our bare hands.

Since our skin and muscles form one of most sophisticated and complex sensory systems, the somatosensory system, the brain can easily interpret the slightest changes and this extra signal processing power gives us a chance to hack into this system by providing artificial inputs. Still, it is rather conspicuous that this is impossible to achieve with today's technology. The essential complication is twofold; the high sensitivity of the very same sensory system makes it difficult to fake or mimic a natural phenomenon by artificial means and on the other hand we don't have a well-defined mapping from the to-be-created sensation to the required excitation signals. Moreover, even if we have such mappings available, the related hardware must execute the computed haptic signal profiles perfectly which is generally not the case.

Then, we could simply ask *Why bother?*

§1.1 The Objectives

We first give an opiniated view about the objectives of the technology and later on, define our microscopic focus of this thesis in this vast generality. This would hopefully give some perspective to what follows in the analysis and synthesis sections.

§1.1.1 *Bilateral Teleoperation*

The touch related applications are diverse. The diversity is not only in terms of sensation they are related to (texture, shape etc.) but also how they encode the information and transmit via various modalities (e.g. vibrational patterns in mobile electronics, variable resistance to motion in game consoles and steering wheels etc.).

§1.1.2 *Objective of This Thesis*

CHAPTER 2

Analysis

§2.1 Introduction

In the last two decades, extensive studies have been published concerning the stability of bilateral teleoperation systems, mainly relying on the conditions which originate from 2-port network theory (see e.g. [**lawrence**, **hannaford89**, **adamshan**, **andersonspong**, **nieslotine**, **yokokohjiyoshikawa**] and also [**hokayemspong**] for a survey). One of the main stability results of network theory is the so-called unconditional stability theorem ([**llewellyn**, **bolinder**]), which states conditions on the network to remain stable whenever connected to any passive immitances on the load and the source side. Therefore, the designer can skip the explicit modeling of the load and the source of a network by just assuming that the terminations are passive. Since interconnection stability of a bilateral teleoperation system driven by a human and exploring a remote environment is analogous to that of a 2-port network, this manner of modeling bilateral teleoperation systems has dominated the literature. In this setting, the human and the environment are assumed to be passive or, more properly, to be represented by passive operators. This allows to test interconnection stability by just applying the unconditional stability theorem. Moreover, if the human and the environment are assumed passive and linear time invariant (LTI), the unconditional stability theorem becomes an exact characterization via Llewellyn's theorem. Therefore, passivity based analysis makes it relatively easy to verify interconnection stability under different environment and human configurations during the interaction. During the last two decades, the passivity assumption became a de facto requirement to perform analysis of teleoperation systems. Even in cases where certain blocks might be active, methods for "passification" of the non-passive interactions have been derived (see e.g. [**ryukwonhanna**]) in which passivity of the blocks is monitored and regulated.

Obviously, this convenience comes with a price. The cost of simplifying the problem is the resulting conservatism of the analysis results. In other words, the proposed tests guarantee stability in the face of an uncertainty set that is often much larger than the set of potential uncertainties that can occur in the physical system. Because of this oversimplified uncertainty structure, worst cases that would not occur in the physical setup are still accounted for. Therefore, an important class of stable interconnections is ruled out due to the conservatism brought in by this assumption. To reduce the involved conservatism, the range of environment dynamics are confined to subsets of all passive LTI operators (e.g. [**adamshan2**, **chopark**, **Peer2008b**, **haddadizaad**, **willaertIJRR10**]).

Another approach was to utilize structured singular value (SSV) tools ([**colgate1**, **colgate2**, **colgate3**, **yokokohjiyoshikawa**, **leungfa**, **kazeroonitsay**, **husalculoewen**, **andrifour**]) to analyze the bilateral teleoperation systems. The main usage was to transform the passive operators to norm-bounded uncertainties via loop transformations which in turn offered a direct handle for the delay problem. Alternatively, a mass-spring-damper system with uncertain coefficients was used to model human/environment for the stability analysis. These studies revealed that it is quite difficult to capture all possible human and environment configurations with a particular LTI uncertainty structure that is compatible with SSV tools. This conclusion has been strongly influenced by two important points: the limitations of the analysis methods that severely restricted the class of allowed uncertainties and the tendency to use an uncertain mechanical system (often of second order) in order to model the human and the environment. These findings led to a diminishing interest in this line of research and to a more intensive focus on the passivity based "modeling avoidance" paradigm in order to circumvent refined modeling issues.

On the other hand, contemporary analysis and synthesis tools in robust control allow us to consider a much larger variety of classes of uncertainties/nonlinearities. Hence, it has become, once again, relevant to strive for a more accurate human model to relax the conservative passivity assumption. Additionally, to the best of our knowledge, the passivity hypothesis on the human is not of fundamental importance.

Note that, when we discuss a possible refined human or environment model, we do not refer to a precise physical model e.g. of the human arm/hand, which is very difficult, if not impossible, to obtain. Instead, we have in mind a model that is represented by a (possibly uncertain) mathematical operator that captures the essential features which remain preserved among individuals, such as constraints on the bandwidth or other bounds on specific properties (directionality, cognitive delay, positioning precision etc.). We would like to emphasize that this can lead to a more complicated family of models than that of a second order mechanical system.

The last fifteen years have witnessed the development of robustness analysis tools based on Integral Quadratic Constraints (IQCs, [**megretski**]) which unify many classical results and which allow to capture time-varying and/or nonlinear uncertainty operators. Despite these improvements it is worth noting that the teleoperation and haptics literature still refers to classical SSV results if addressing the issues of robustness. In some places, the terminology of nominal performance, robust stability and robust performance is used interchangeably (e.g. $\mathcal{H}_\infty$ vs. μ). This reveals that there is only a limited tendency to utilize these more advanced IQC tools in the teleoperation community. Still, after a hiatus of explicit use of robust control techniques, the number of studies for teleoperation along this direction has been increasing (see e.g. [**poorten**, **boukhnifer**, **naghsh**, **kimcavusoglu**] and references therein to name a few among many others).

In this paper, which has been partially presented in [**polatACC11**, **polatIFAC11**, **polatWH11**], stability conditions from network theory are reformulated in terms of quadratic constraints. Their equivalence is shown to emphasize that the analysis and synthesis problems can be carried over to the robust control framework without giving away the exactness of the conditions and without relying on the particular terminology of network theory or that of electrical engineering in general. Our main purpose is to unify the existing frequency domain analysis tools in a systematic way and, furthermore, to point out the underlying connections explicitly.

Based on this formulation, we show how one can extend the stability analysis to cases that are excluded by the hypotheses of the classical tools and we provide illustrations by numerical examples. As another important advantage of this approach, it allows for a fair comparison of various control design algorithms that have been proposed in the teleoperation literature. We present a convenient framework that can be utilized to assess, for example, the properties of different controllers as discussed in [**hzaadsalcu**, **rodriseda**].

The notation is standard. $\mathcal{L}_2^n$ is the space of $\mathbb{R}^n$-valued square summable functions on $(0,\infty)$, the extended real line is $\mathbb{R}_e := \mathbb{R}\cup\{\infty\}$ and a hat $\hat{f}$ denotes the Fourier transform of f. For Hermitian matrices $M \succ 0$, $M \prec 0$ ($M \succeq 0$, $M \preceq 0$) means positive and negative (semi) definiteness respectively. The symbol $\star$ is used as a placeholder to save space, such as in $(\star)^* QN$ which means N^*QN. $\mathcal{RH}_\infty$ ($\mathcal{RH}_\infty^{\bullet\times\bullet}$) denotes the set of real rational, proper and stable transfer functions (matrices) and $\|G\|_\infty$ is the H_∞-norm, the largest singular value of $G \in \mathcal{RH}_\infty^{\bullet\times\bullet}$ over frequency. An upper (lower) linear fractional transformation (LFT) is denoted by $\Delta \star G = G_{22} + G_{21}\Delta(I - G_{11}\Delta)^{-1}G_{12}$ ($G \star \Delta = G_{11} + G_{12}\Delta(I - G_{22}\Delta)^{-1}G_{21}$) with an appropriate partitioning of G. State-space realizations $G(s) = C(sI - A)^{-1}B + D$ are denoted as $G = \left[\begin{array}{c|c} A & B \\ \hline C & D \end{array}\right]$.

§2.2 Preliminaries

In this section, we will briefly give a technical overview of the multiplier methods to base our discussion on and to relate to the passivity based results. Let us first consider the system representations that we will employ throughout the paper.

§2.2.1 *System Representations*

In network theory and also in its application to bilateral teleoperation, the "system" refers to the network model that is hypothetically disconnected (thus admitting virtual terminals) from its "surroundings" such as the "load" and the "source" of a circuit. This system is allowed to interact with its surroundings via "ports" or, more generally, circuit terminal pairings that satisfy some technical assumptions. In the teleoperation context, if one uses the "load-source" analogy for the manipulated environment and the human, then the system models all the bilateral interaction between the load and the source ports (as in Figure **??**). Furthermore, by imposing an artificial causality scheme,

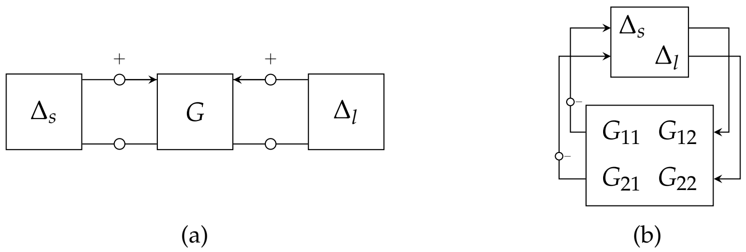

Figure 2.1: Two representations of a 2-port network.

two of these signals can be selected as free variables and the remaining ones become dependent variables ([**behavbook**]). Depending on the choice of the free variables, the system can be expressed in terms of impedance, admittance and hybrid parameters for 2-port networks and their combinations for general n-port network interconnections. With a slight abuse of notation, we will use the term “immitance" matrix to refer to any of these representations. Suppose that a 2-port immitance matrix is partitioned as

$$\begin{pmatrix} q \\ y \end{pmatrix} = \begin{pmatrix} G_1 & G_2 \\ G_3 & G_4 \end{pmatrix} \begin{pmatrix} p \\ u \end{pmatrix}$$

where q, y, p, u represent the flow and the effort signals. Then, obtaining one representation from another is possible by a combination of the following elementary “permutation" and “partial inversion" operations:

$$\begin{pmatrix} q \\ y \end{pmatrix} = \begin{pmatrix} G_2 & G_1 \\ G_4 & G_3 \end{pmatrix} \begin{pmatrix} u \\ p \end{pmatrix}, \qquad \text{(Permutation)}$$

$$\begin{pmatrix} p \\ y \end{pmatrix} = \begin{pmatrix} G_1^{-1} & -G_1^{-1}G_2 \\ G_3G_1^{-1} & G_4 - G_3G_1^{-1}G_2 \end{pmatrix} \begin{pmatrix} q \\ u \end{pmatrix}. \qquad \text{(Partial Inversion)}$$

(In the latter operation it is assumed that the inverse exists.) For our purposes, we consider only the immitance matrices that describe G as an input-output mapping (as opposed to transmission or ABCD parameters) as follows:

$$\begin{pmatrix} q \\ y \end{pmatrix} = \begin{pmatrix} G_1 & G_2 \\ G_3 & G_4 \end{pmatrix} \begin{pmatrix} p \\ u \end{pmatrix}, \quad \begin{pmatrix} p \\ u \end{pmatrix} = \begin{pmatrix} \Delta_s & 0 \\ 0 & \Delta_l \end{pmatrix} \begin{pmatrix} q \\ y \end{pmatrix}. \tag{2.1}$$

Therefore, the overall interconnection can be depicted by the block diagram given in Figure **??**. In relation to teleoperation, the blocks Δ_s and Δ_l refer to the human and the unknown environment. Throughout the paper, we will not distinguish the system G from its transfer matrix $G(s)$ unless specifically stated otherwise.

Remark 1. *When a port representation is replaced with an input/output representation, the flow variable, such as e.g. the electric current, requires a sign change relative to the "from" and "to" ports in order to indicate the travel direction. This ambiguity is typically resolved by interconnecting systems with a negative sign in the loop, which causes the difference between Figure* **??** *and Figure* **??**.

Figure 2.2: The general interconnection (left) and the assumed interconnection for passive systems (right)

§2.2.2 *Passivity, Well posedness and Stability*

Let us start by recalling the key concept of passivity.

Definition 1. *Let an operator $G : \mathcal{L}_2^n \to \mathcal{L}_2^n$ be given. G is said to be passive if the following condition holds for all $u \in \mathcal{L}_2^n$:*

$$\int_0^\infty G(u)(\tau)^T u(\tau) d\tau = \int_{-\infty}^\infty \widehat{G(u)}(i\omega)^* \hat{u}(i\omega) d\omega \geq 0.$$

For an LTI operator G, passivity is equivalent to the corresponding transfer function $G(s)$ being positive real:

$$\begin{aligned} \operatorname{Re}\{G(i\omega)\} \geq 0 &\Longleftrightarrow \hat{u}^*(i\omega) \operatorname{Re}\{G(i\omega)\} \hat{u}(i\omega) \geq 0 \\ &\Longleftrightarrow \int_{-\infty}^\infty \hat{u}^*(i\omega) \operatorname{Re}\{G(i\omega)\} \hat{u}(i\omega) d\omega \geq 0 \\ &\Longleftrightarrow \int_{-\infty}^\infty [G(i\omega)\hat{u}(i\omega)]^* \hat{u}(i\omega) d\omega \geq 0 \end{aligned}$$

for all $\omega \in \mathbb{R}_e$ and for all $u \in \mathcal{L}_2^n$. Furthermore, if the condition

$$\int_0^\infty G(u)(\tau)^T u(\tau) d\tau \geq \delta \|u\|_2^2 + \epsilon \|G(u)\|_2^2$$

is satisfied with $\delta > 0$, $\epsilon = 0$ (or $\delta = 0$, $\epsilon > 0$) then the operator is said to be Strictly Input (Output) Passive with level δ (or level ϵ) respectively. Let us now recall the basic notions of well-posedness and stability and present two celebrated stability theorems.

Definition 2. *Consider the interconnection depicted in Figure **??** with $G, \Delta \in \mathcal{RH}_\infty^{\bullet\times\bullet}$ of compatible dimensions. This $G - \Delta$ interconnection is said to be well-posed if $(I - G\Delta)(s)$ has a proper inverse. Moreover, the interconnection is said to be stable if it is well-posed and if the inverse of $(I - G\Delta)(s)$ is stable.*

These definitions do as well apply to the negative feedback interconnection of G_p and Δ in Figure **??** by just replacing G with $-G_p$.

Theorem 1. *[Passivity] The $G_p - \Delta$ interconnection in Figure **??** for LTI systems $G_p, \Delta \in \mathcal{RH}_\infty^{\bullet\times\bullet}$ is stable for all passive Δ if and only if G_p is strictly input passive.*

Theorem 2. *[Small-Gain] The $G - \Delta$ interconnection in Figure **??** for LTI systems $G, \Delta \in \mathcal{RH}_\infty^{\bullet\times\bullet}$ is stable for all Δ with $\|\Delta\|_\infty \leq 1$ if and only if $\|G\|_\infty < 1$.*

§2.2.3 *Quadratic Forms for Stability Analysis*

In the sequel, instead of 2-port networks, we rather consider system interconnections as depicted in Figure **??**. In this setting, G is the model of the nominal bilateral teleoperation system and Δ is a block diagonal collection of uncertainties, such as the human, the environment, delays etc. Stability tests are based on structural hypotheses on the diagonal blocks of the operator Δ such as gain-bounds or passivity. These properties should allow to develop numerically verifiable conditions for the system G that guarantee interconnection stability. This is intuitive because we have no access to the actual Δ and we can only describe its blocks by means of indirect properties. During the last three decades many classical stability results have been unified and generalized in this direction by utilizing quadratic forms ([**safonov**, **carsten2**, **iwasaki**, **megretski**]).

It is beyond the scope of this paper to include a comprehensive treatment of the subject, but for the sake of completeness, we present the general methodology by sampling a few important special cases. To begin with, consider the following reformulation of the conditions of the small gain theorem:

$$\begin{matrix} \|\Delta\|_\infty \leq 1 \\ \|G\|_\infty < 1 \end{matrix} \iff \begin{matrix} \begin{pmatrix} \Delta(i\omega) \\ 1 \end{pmatrix}^* \begin{pmatrix} -1 & 0 \\ 0 & 1 \end{pmatrix} \begin{pmatrix} \Delta(i\omega) \\ 1 \end{pmatrix} \succeq 0 \\ \begin{pmatrix} 1 \\ G(i\omega) \end{pmatrix}^* \begin{pmatrix} -1 & 0 \\ 0 & 1 \end{pmatrix} \begin{pmatrix} 1 \\ G(i\omega) \end{pmatrix} \prec 0 \end{matrix} \tag{2.2}$$

for all $\omega \in \mathbb{R}_e$. The middle 2×2-matrix on the right-hand side is called the "*multiplier*" (typically denoted by Π). It has been observed that the appearance of the same multiplier on both inequalities is far from a mere coincidence. In fact, it led to the following stability test: Assume that $G, \Delta \in \mathcal{RH}_\infty^{\bullet\times\bullet}$. Then, the $G - \Delta$ interconnection in Figure **??** is well-posed and stable if there exists a Hermitian matrix Π such that

$$\begin{pmatrix} \Delta(i\omega) \\ I \end{pmatrix}^* \Pi \begin{pmatrix} \Delta(i\omega) \\ I \end{pmatrix} \succeq 0 \tag{2.3}$$

$$\begin{pmatrix} I \\ G(i\omega) \end{pmatrix}^* \Pi \begin{pmatrix} I \\ G(i\omega) \end{pmatrix} \prec 0 \tag{2.4}$$

hold for all $\omega \in \mathbb{R}_e$; one only requires the mild technical hypothesis that the left-upper/right-lower block of Π is negative/positive semi-definite. Thus, the intuition that we touched upon above is mathematically formalized by (**??**) and (**??**). Indeed, one can see that the former condition constrains the family of uncertainties while the latter provides the related condition imposed on the plant for interconnection stability, both expressed in terms of the multiplier Π. In particular, we recover the passivity theorem in a similar fashion, if using the constant symmetric matrix $\Pi = \left(\begin{smallmatrix} 0 & I \\ I & 0 \end{smallmatrix}\right)$ as the multiplier under negative feedback. The interested reader is referred to [**safonov**] for a lucid "topological seperation" argument. Various other classical stability tests fall under this particular scenario based on the so-called static (frequency-independent) multipliers which, therefore, presents a significantly unified methodology.

If Δ admits a diagonal structure (as in Figure **??**) it is well known that the small-gain theorem and passivity theorem are conservative. A natural generalization towards a tighter analysis test is using a frequency dependent Π matrix, which can be interpreted as adding dynamics to the multiplier. Two prominent examples of interest are the celebrated upper bound computations for μ or κ_m in robust control theory and, as we will show later, Llewellyn's stability conditions. As a shortcoming, these results are only valid for LTI operators but the real power and flexibility of these multiplier methods come from their generalizations to classes of nonlinear/time-varying operators via the IQC framework that appeared in [**megretski**].

An Integral Quadratic Constraint (IQC) for the input and output signals of Δ is expressed as

$$\int_{-\infty}^{\infty} \begin{pmatrix} \widehat{\Delta(v)}(i\omega) \\ \hat{v}(i\omega) \end{pmatrix}^{*} \Pi(i\omega) \begin{pmatrix} \widehat{\Delta(v)}(i\omega) \\ \hat{v}(i\omega) \end{pmatrix} d\omega \geq 0. \tag{2.5}$$

A bounded operator $\Delta : \mathcal{L}_2^m \to \mathcal{L}_2^n$ is said to satisfy the constraint defined by $\Pi(i\omega)$ if (**??**) holds for all $v \in \mathcal{L}_2^m$. The following sufficient stability condition for the interconnection in Figure **??** is the main theorem which forms the basis for the IQC framework.

Theorem 3 ([**megretski**])**.** *Let the system model $G \in \mathcal{RH}_\infty^{n\times m}$ be given and let $\Delta : \mathcal{L}_2^m \to \mathcal{L}_2^n$ be a bounded causal operator. Suppose that*

1. *for every $\tau \in [0,1]$, the interconnection of G and $\tau\Delta$ is well-posed;*
2. *for every $\tau \in [0,1]$, $\tau\Delta$ satisfies the IQC defined by $\Pi(i\omega)$ which is bounded as a function of $\omega \in \mathbb{R}$;*
3. *there exists some $\epsilon > 0$ such that*

$$\begin{pmatrix} I \\ G(i\omega) \end{pmatrix}^{*} \Pi(i\omega) \begin{pmatrix} I \\ G(i\omega) \end{pmatrix} \preceq -\epsilon I \text{ for all } \omega \in \mathbb{R}. \tag{2.6}$$

*Then the $G - \Delta$ interconnection in Figure **??** is stable.*

Remark 2.

- *We observe that both 1) and 2) in Theorem **??** have to hold for all scaled versions $\tau\Delta$, $\tau \in [0,1]$, of the uncertainty block in order to allow for general multipliers Π that are merely required to be bounded on the imaginary axis.*
- *In our examples the left-upper $m \times m$-block of $\Pi(i\omega)$ is negative semi-definite and the right-lower $n \times n$-block is positive semi-definite for all $\omega \in \mathbb{R}_e$. It is then easy to see that (**??**) implies Property 2) in Theorem **??**; hence one only needs to verify (**??**) for the original uncertainty Δ.*
- *Often $\Pi(i\omega)$ is a continuous function of $\omega \in \mathbb{R}_e$. Then Property 3) is equivalent to*

$$\begin{pmatrix} I \\ G(i\omega) \end{pmatrix}^{*} \Pi(i\omega) \begin{pmatrix} I \\ G(i\omega) \end{pmatrix} \prec 0 \text{ for all } \omega \in \mathbb{R}_e. \tag{2.7}$$

- *If Δ is LTI then* (**??**) *holds for all $v \in \mathcal{L}_2^m$ if and only if*

$$\begin{pmatrix} \Delta(i\omega) \\ I \end{pmatrix}^* \Pi(i\omega) \begin{pmatrix} \Delta(i\omega) \\ I \end{pmatrix} \succeq 0 \text{ for all } \omega \in \mathbb{R}. \tag{2.8}$$

The IQC reduces to a frequency-domain inequality (FDI). This provides the link to our introductory discussion.

- *Suppose that Δ is LTI and $\Pi(i\omega)$ is a continuous function of $\omega \in \mathbb{R}_e$. It is not difficult to show that* (**??**) *and* (**??**) *imply*

$$\det(I - G(i\omega)\Delta(i\omega)) \neq 0 \text{ for all } \omega \in \mathbb{R}_e, \tag{2.9}$$

*which is the precise condition that forms the basis of SSV theory [**packdoyle**]. This gives some intuition for the validity of the IQC theorem and relates to μ in SSV-theory.*

In combination with the previous remarks, Properties 2) and 3) imply $\det(I - \tau G(\infty)\Delta(\infty)) \neq 0$ for $\tau \in [0, 1]$ which is nothing but 1). Two conclusion can be drawn: On the one hand, under these circumstances Property 1) is redundant in Theorem **??**. *On the other hand, if 1) and 2) have been verified, it suffices to check* (**??**) *only for finite $\omega \in \mathbb{R}$ in order to infer stability with the IQC theorem.*

If we have found an IQC constraint that is satisfied for all $\Delta \in \mathbf{\Delta}$ with some particular uncertainty set $\mathbf{\Delta}$, checking robust stability boils down to the verification of the corresponding FDI (**??**) or (**??**). Instead of checking these in a frequency-by-frequency fashion, one can make use of the Kalman-Yakubovich-Popov (KYP) Lemma (see [**rantzerkyp**]) in order to convert the FDI into a genuine Linear Matrix Inequality (LMI) by using state space representations.

Theorem 4 (KYP Lemma)**.** *Let $G(s) = \left[\begin{array}{c|c} A & B \\ \hline C & D \end{array}\right]$ and suppose that A has no eigenvalues on the imaginary axis. For a given symmetric matrix P, the following two statements are equivalent:*

1. *The following FDI holds:*

$$G(i\omega)^* P G(i\omega) \succ 0 \;\; \forall \omega \in \mathbb{R}_e. \tag{2.10}$$

2. *There exists a symmetric matrix X with*

$$\left(\begin{array}{cc} I & 0 \\ A & B \\ \hline C & D \end{array}\right)^T \left(\begin{array}{cc|c} 0 & X & 0 \\ X & 0 & 0 \\ \hline 0 & 0 & P \end{array}\right) \left(\begin{array}{cc} I & 0 \\ A & B \\ \hline C & D \end{array}\right) \succ 0. \tag{2.11}$$

For the finite frequency intervals, one can further use the Generalized KYP Lemma ([**genelKYP**]) to limit the analysis to some physically relevant frequency band.

§2.3 Equivalent IQC stability tests for common stability analysis approaches

In this section, we present the equivalent IQC tests for some widely used results from network theory. Our main motivation is to show the underlying basic connection to the IQC framework. It is revealed that the frequency domain stability tests in the context of bilateral teleoperation can be seen as particular cases of robustness tests with suitable multipliers. This reformulation forms the basis for substantial extensions as discussed later in the paper.

Subsequently, we will present proofs of sufficiency and only include some brief remarks about necessity (exactness) of these tests in Section **??**.

§2.3.1 *Llewellyn Stability Criteria*

The well known conditions for stability of a two-port network, formulated in [**llewellyn**, **bolinder**, **rollett**], are recalled in the following theorem. An explicit indication of the frequency dependence is often omitted for notational convenience.

Theorem 5 (Llewellyn's Criteria). *A 2-port network N, described by its transfer matrix*

$$N(i\omega) = \begin{pmatrix} N_{11}(i\omega) & N_{12}(i\omega) \\ N_{21}(i\omega) & N_{22}(i\omega) \end{pmatrix}$$

and interconnected to passive termination immitances as in Figure **??**, *is stable if and only if*

$$R_{11} > 0 \text{ or } R_{22} > 0, \tag{2.12}$$

and

$$4\left(R_{11}R_{22} + X_{12}X_{21}\right)\left(R_{11}R_{22} - R_{12}R_{21}\right) - \left(R_{12}X_{21} - R_{21}X_{12}\right)^2 > 0 \tag{2.13}$$

or

$$2R_{11}R_{22} - |N_{12}N_{21}| - \text{Re}\left\{N_{12}N_{21}\right\} > 0 \tag{??'}$$

for all $\omega \in \mathbb{R}_e$, where R_{ij} and X_{ij} denote the real and imaginary parts of N_{ij} respectively.

Remark 3. *This result is also presented with non-strict inequalities in the literature. However, non-strict inequalities do not guarantee asymptotic interconnection stability (as considered all throughout this paper) but only lead to certain passivity properties of the interconnection (see [*__khalil__*] and [*__lawrence__*]).*

As shown in [**rollett**], the conditions stated in Theorem **??** are invariant under immitance substitution. Hence, we assume that the network and the terminations are represented with an input/output mapping as depicted in Figure **??**.

The stability conditions of Theorem **??** can be reproduced via the IQC theorem as follows. If Δ_l and Δ_s are passive and stable LTI systems, they satisfy

$$\Delta_l + \Delta_l^* \geq 0 \text{ and } \Delta_s + \Delta_s^* \geq 0$$

for all $\omega \in \mathbb{R}_e$. If we choose arbitrary $\lambda_1(\omega) > 0$ and $\lambda_2(\omega) > 0$, it is clear that the inequalities

$$\begin{aligned} \lambda_1(\Delta_s + \Delta_s^*) \geq 0 \\ \lambda_2(\Delta_l + \Delta_l^*) \geq 0 \end{aligned}$$

persist to hold, which in turn can be combined into

$$\left(\begin{array}{cc} \Delta_s & 0 \\ 0 & \Delta_l \\ \hline 1 & 0 \\ 0 & 1 \end{array}\right)^* \left(\begin{array}{cc|cc} 0 & 0 & \lambda_1 & 0 \\ 0 & 0 & 0 & \lambda_2 \\ \hline \lambda_1 & 0 & 0 & 0 \\ 0 & \lambda_2 & 0 & 0 \end{array}\right) \left(\begin{array}{cc} \Delta_s & 0 \\ 0 & \Delta_l \\ \hline 1 & 0 \\ 0 & 1 \end{array}\right) \succeq 0.$$

After division by $\lambda_2(\omega)$ and with $\lambda(\omega) = \frac{\lambda_1(\omega)}{\lambda_2(\omega)}$ we obtain

$$\left(\begin{array}{cc} \Delta_s & 0 \\ 0 & \Delta_l \\ \hline 1 & 0 \\ 0 & 1 \end{array}\right)^* \left(\begin{array}{cc|cc} 0 & 0 & \lambda & 0 \\ 0 & 0 & 0 & 1 \\ \hline \lambda & 0 & 0 & 0 \\ 0 & 1 & 0 & 0 \end{array}\right) \left(\begin{array}{cc} \Delta_s & 0 \\ 0 & \Delta_l \\ \hline 1 & 0 \\ 0 & 1 \end{array}\right) \succeq 0. \tag{2.14}$$

In this fashion we have constructed a whole family of multipliers, parameterized by $\lambda(\omega) > 0$, such that the quadratic constraint (**??**) holds for all passive $\Delta_l, \Delta_s \in \mathcal{RH}_\infty$. Stability of the $N - \Delta$ interconnection is then guaranteed if one can find a positive $\lambda(\omega)$ such that the corresponding frequency domain inequality

$$(\star)^* \left(\begin{array}{cc|cc} 0 & 0 & \lambda & 0 \\ 0 & 0 & 0 & 1 \\ \hline \lambda & 0 & 0 & 0 \\ 0 & 1 & 0 & 0 \end{array}\right) \left(\begin{array}{cc} 1 & 0 \\ 0 & 1 \\ \hline -N_{11} & -N_{12} \\ -N_{21} & -N_{22} \end{array}\right) \prec 0 \tag{2.15}$$

is also satisfied at each frequency $\omega \in \mathbb{R}_e$ (Negation of N results from the application of the IQC theorem to the negative feedback interconnection Figure **??**). The resulting condition is equivalent to checking whether, at each frequency, there exists a $\lambda > 0$ such that

$$H = \begin{bmatrix} -2\lambda R_{11} & -\lambda N_{12} - N_{21}^* \\ -\lambda N_{12}^* - N_{21} & -2R_{22} \end{bmatrix} \prec 0$$

holds. This leads us to the relation with the classical results. Indeed, the 2×2 matrix H is negative definite if and only if

$$R_{11} > 0 \quad \text{or} \quad R_{22} > 0$$

and

$$\det H = \left(-R_{12}^2 - X_{12}^2\right)\lambda^2 - R_{21}^2 - X_{21}^2 + \left(4R_{11}R_{22} - 2R_{12}R_{21} + 2X_{12}X_{21}\right)\lambda > 0.$$

Since the leading and constant coefficient of the involved polynomial are negative, the apex of the corresponding parabola should stay above the λ-axis. Using the apex coordinates of a concave parabola one can show that this is equivalent to (**??**). Symmetry of the resulting conditions with respect to the indices is shown by simply switching the roles of λ_1 and λ_2 in our derivation.

Remark 4. *In the previous FDI condition* (**??**) *and if assuming $\lambda = 1$ over all frequencies, we also recover the passivity theorem or Raisbeck's conditions [***raisbeck***]. A comparison of Raisbeck's and Llewellyn's criteria indicates that the use of frequency dependent multipliers demonstrates the possibility of a substantial decrease of conservatism in stability analysis. In fact, the difference between Llewellyn's remarkable conditions and of Raisbeck's is the use of a dynamic multiplier $\left(\begin{smallmatrix} 0 & \lambda \\ \lambda & 0 \end{smallmatrix}\right)$ instead of the static one with $\lambda = 1$.*

Remark 5. *One should also note that Llewellyn's original conditions are both sufficient and necessary and, hence, involve no conservatism. Exactness is due to the vast generality of the uncertainties, since one just assumes that the human and the environment are represented by passive LTI operators. The Nyquist curves of the corresponding positive real functions are only constrained to be lying in the closed right half plane. In reality, however, one is rather interested in operators whose Nyquist curves are confined to a sub-region of the closed right-half plane (or even to other bounded sets elsewhere in the complex plane). Covering the relevant region of interest in the complex plane with the full closed right-half plane for describing the involved uncertainty provides a clear account of the conservatism of the stability tests in teleoperation systems, as often mentioned in the literature. Thus, if one wishes to reduce conservatism, additional structural information about the operators should be included in order to further constrain the uncertainty set. It will be illustrated in Section* **??** *how this can be achieved by using conic combinations of different multipliers which express refined properties of the involved operators.*

§2.3.2 *Unconditional Stability Analysis of 3-port Networks*

Recently, in [**khademian**] and references therein, Llewellyn's analysis method has been applied to three port networks. The main idea is to obtain a 2-port network by terminating one of the ports with a known environment model and then apply the test on the resulting particular 2-port network. We will obtain the exact conditions for unconditional stability of a 3-port in a straightforward fashion along the above described lines without port termination. We include this discussion in order to illustrate that it is still simple to obtain stability conditions for situations in which no obvious circuit theoretical analogues exist. As expected, the test derived in this section is more conservative than that of [**khademian**] since the authors include additional information about the model with which the port is terminated, that renders their uncertainty set significantly smaller.

If compared to the previous section, the only modification is to take a system representation $N \in \mathcal{RH}_\infty^{3\times 3}$ and three passive uncertainty blocks living in $\mathcal{RH}_\infty$ which are collected as

$$\Delta(i\omega) = \operatorname{blkdiag}\left(\Delta_1(i\omega), \Delta_2(i\omega), \Delta_3(i\omega)\right) \tag{2.16}$$

in order to model the three port terminations. With

$$\Lambda(i\omega) = \operatorname{blkdiag}\left(\lambda_1(\omega), \lambda_2(\omega), \lambda_3(\omega)\right) \succ 0 \tag{2.17}$$

we obtain the following quadratic constraint

$$\begin{pmatrix} \Delta \\ I \end{pmatrix}^* \begin{pmatrix} 0 & \Lambda \\ \Lambda & 0 \end{pmatrix} \begin{pmatrix} \Delta \\ I \end{pmatrix} \succeq 0$$

which reflects passivity of the three sub-blocks. The corresponding FDI for guaranteeing stability reads as

$$\begin{pmatrix} I \\ -N \end{pmatrix}^* \begin{pmatrix} 0 & \Lambda \\ \Lambda & 0 \end{pmatrix} \begin{pmatrix} I \\ -N \end{pmatrix} \prec 0. \tag{2.18}$$

We arrive at the following 3-port unconditional stability condition.

Theorem 6 (Llewellyn's 3-port Criteria). *A network, represented by its 3×3 transfer function $N \in \mathcal{RH}_\infty^{3\times 3}$ and interconnected to the stable, passive and block diagonal Δ as given in (**??**) is stable if and only if there exists a structured Λ with (**??**) such that (**??**) holds for all $\omega \in \mathbb{R}_e$.*

Exact conditions for unconditional stability could be obtained from (**??**) by symbolic computations. However, getting formulas similar to those in (**??**), (**??**) would lead to quite cumbersome expressions (see e.g. [**kuochu**, **tan**, **khademian**]). Moreover, variants of expressing negative definiteness would result in different formulations of the stability conditions in terms of scalar inequalities. In the IQC formulation this is completely avoided while it is still possible to easily verify the resulting conditions numerically.

§2.3.3 *Rollett's Stability Condition*

Similarly, as is for Llewellyn's stability conditions, it is straightforward to derive unconditional stability tests if the network is represented by scattering parameters. In what follows, we denote transformed passive LTI uncertainties with $\tilde{\Delta}_s, \tilde{\Delta}_l$ which are unity gain bounded. The corresponding interconnection is supposed to be given by the loop equations $q = Sp$, $p = \tilde{\Delta} q$ i.e.

$$\begin{pmatrix} q_1 \\ q_2 \end{pmatrix} = \begin{pmatrix} S_{11} & S_{12} \\ S_{21} & S_{22} \end{pmatrix} \begin{pmatrix} p_1 \\ p_2 \end{pmatrix}, \quad \begin{pmatrix} p_1 \\ p_2 \end{pmatrix} = \begin{pmatrix} \tilde{\Delta}_s & 0 \\ 0 & \tilde{\Delta}_l \end{pmatrix} \begin{pmatrix} q_1 \\ q_2 \end{pmatrix}. \tag{2.19}$$

Rollett's conditions ([**stern**, **rollett**, **kurokawa**]) for stability are then formulated as follows: The inequality

$$K = \frac{1 + |\nabla|^2 - |S_{11}|^2 - |S_{22}|^2}{2\,|S_{12}S_{21}|} > 1 \tag{2.20}$$

holds for all frequencies together with an auxiliary condition expressed in terms of $\nabla = S_{11}S_{22} - S_{12}S_{21}$. This extra condition can be stated in at least five different ways, such as e.g.

$$1 - |S_{11}|^2 > |S_{12}S_{21}| \quad \text{or} \quad (1 - |S_{22}|^2) > |S_{12}S_{21}|\,.$$

(See [**edsin**] for further details). With almost identical arguments as for Llewellyn's test, one derives the following quadratic constraints for positive λ and for stable LTI systems $\tilde{\Delta}_l$ and $\tilde{\Delta}_s$ whose gains are bounded by one:

$$\left(\begin{array}{cc} \tilde{\Delta}_s & 0 \\ 0 & \tilde{\Delta}_l \\ \hline 1 & 0 \\ 0 & 1 \end{array}\right)^* \left(\begin{array}{cc|cc} -\lambda & 0 & & \\ 0 & -1 & & \\ \hline & & \lambda & 0 \\ & & 0 & 1 \end{array}\right) \left(\begin{array}{cc} \tilde{\Delta}_s & 0 \\ 0 & \tilde{\Delta}_l \\ \hline 1 & 0 \\ 0 & 1 \end{array}\right) \succeq 0.$$

Interconnection stability is then assured if one can find a positive frequency dependent λ for which the FDI

$$\left(\begin{array}{cc} 1 & 0 \\ 0 & 1 \\ \hline S_{11} & S_{12} \\ S_{21} & S_{22} \end{array}\right)^* \left(\begin{array}{cc|cc} -\lambda & 0 & & \\ 0 & -1 & & \\ \hline & & \lambda & 0 \\ & & 0 & 1 \end{array}\right) \left(\begin{array}{cc} 1 & 0 \\ 0 & 1 \\ \hline S_{11} & S_{12} \\ S_{21} & S_{22} \end{array}\right) \prec 0 \tag{2.21}$$

or, equivalently,

$$H = \begin{bmatrix} |S_{21}|^2 + \lambda(|S_{11}|^2 - 1) & S_{22}S_{21}^* + \lambda S_{12}S_{11}^* \\ S_{22}^*S_{21} + \lambda S_{12}^*S_{11} & |S_{22}|^2 - 1 + \lambda\,|S_{12}|^2 \end{bmatrix} \prec 0$$

hold for all $\omega \in \mathbb{R}_e$. Then, it is elementary to express $H \prec 0$ by $\det(H) > 0$ and by negativity of the diagonal entries of H for all $\omega \in \mathbb{R}_e$. Positivity of the determinant of H means

$$(1 - |S_{22}|^2 - |S_{11}|^2 + |\nabla|^2)\lambda - |S_{12}|^2\,\lambda^2 - |S_{21}|^2 > 0.$$

If this is expressed as $f(\lambda) = -a\lambda^2 + b\lambda - c > 0$ with $a, c > 0$, we require the apex coordinates $\left(\frac{b}{2a}, \frac{b^2-4ac}{4a}\right)$ both to be positive. Since $a > 0$, we have

$$(1 + |\nabla|^2 - |S_{22}|^2 - |S_{11}|^2)^2 > 4\,|S_{12}S_{21}|^2 \tag{2.22}$$

due to $b^2 > 4ac$. Moreover, negativity of the diagonal terms is expressed as

$$\lambda(1 - |S_{11}|^2) > |S_{21}|^2 \quad \text{or} \quad 1 - |S_{22}|^2 > \lambda\,|S_{12}|^2\,. \tag{2.23}$$

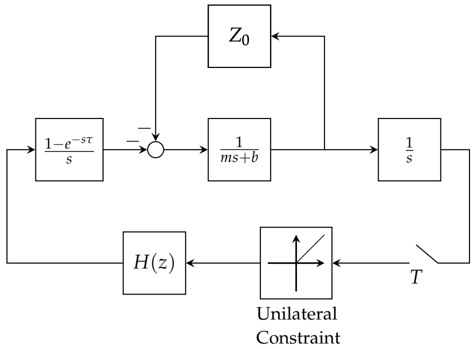

Figure 2.3: The teleoperation setup from [**colgate1**]

To make the connection to the classical auxiliary conditions, observe that evaluating $f(\lambda)$ at $\lambda_0 = \sqrt{\frac{c}{a}} = \frac{|S_{21}|}{|S_{12}|}$ would lead to the condition $b > 0$ since $f(\lambda_0) = b\sqrt{\frac{c}{a}} - 2c > 0$. Hence (**??**) becomes

$$1 - |S_{11}|^2 > |S_{12}S_{21}| \quad \text{or} \quad 1 - |S_{22}|^2 > |S_{12}S_{21}|\,. \tag{2.24}$$

In the literature, the quantity λ_0 is called the "maximum stable power gain". Finally, after explicitly including the condition $b > 0$, one can take the square root of (**??**) and obtain

$$1 + |\nabla|^2 - |S_{22}|^2 - |S_{11}|^2 > 2\,|S_{12}S_{21}|\,,$$

which is precisely Rollett's first condition.

There has been quite some discussion in various studies (e.g. [**lombardi**, **edsin**, **woods**, **pirola**]) whether testing both conditions in (**??**) is really required, while it rolls out from our FDI arguments that one of these auxiliary inequalities is sufficient. In fact, (**??**) renders this discussion obsolete since we deal with a single matrix inequality to be tested at each frequency. This test is equivalent to the one based on the Edwards-Sinsky stability parameter μ ([**edsin**]) in the sense that only one condition needs to be verified. Alternatively, one can perform a symbolic computation of the largest eigenvalue of H and search for a positive λ that renders that quantity strictly negative. Recently, the μ parameter has been used in the context of teleoperation in [**haddadizaad**] and their results can also be recovered by using multipliers similar to the ones given in the next section.

§2.3.4 *Colgate's Minimum Damping Condition*

In this section, the analysis problem from [**colgate2**, **colgate6**] is investigated by IQCs. In this example, the master device is modeled as $\frac{1}{ms+b}$ and is combined with a passive operator impedance $Z_0(s)$ as shown in Figure **??**. We limit the analysis to the situation without the unilateral constraint. The overall operator and master device transfer function reads as

$$\Delta(s) = \frac{1}{ms + b + Z_0(s)}.$$

Since $Z_0(s)$ is passive and b is positive, the Nyquist curve of $\Delta^{-1}(s)$ is confined to the half-plane $\{z \in \mathbb{C} : \mathrm{Re}\{z\} \geq b\}$ and $\Delta^{-1}(s)$ is strictly input passive with parameter $2b$. In [**colgate2**], the problem is converted to the small gain theorem with a geometric reasoning. In our setting, the passivity property is expressed as

$$\begin{pmatrix} 1 \\ \Delta(i\omega)^{-1} \end{pmatrix}^* \begin{pmatrix} -2b & 1 \\ 1 & 0 \end{pmatrix} \begin{pmatrix} 1 \\ \Delta(i\omega)^{-1} \end{pmatrix} \geq 0$$

which is clearly equivalent to

$$\begin{pmatrix} \Delta(i\omega) \\ 1 \end{pmatrix}^* \begin{pmatrix} -2b & 1 \\ 1 & 0 \end{pmatrix} \begin{pmatrix} \Delta(i\omega) \\ 1 \end{pmatrix} \geq 0$$

for all $\omega \in \mathbb{R}_e$. The FDI guaranteeing stability then reads as

$$\begin{pmatrix} 1 \\ -G_d(i\omega) \end{pmatrix}^* \begin{pmatrix} -2b & 1 \\ 1 & 0 \end{pmatrix} \begin{pmatrix} 1 \\ -G_d(i\omega) \end{pmatrix} < 0$$

Using the closed form formula in [**colgate2**],

$$G_d(i\omega) = \frac{T}{2} \frac{e^{i\omega T} - 1}{1 - \cos(\omega T)} H(e^{i\omega T})$$

this inequality leads directly to Colgate's original condition which read as

$$\begin{aligned} &-2b - G_d^*(i\omega) - G_d(i\omega) < 0 \\ &\qquad\qquad \iff b > \frac{T}{2} \frac{1}{1 - \cos(\omega T)} \mathrm{Re}\left\{(1 - e^{-i\omega T}) H(e^{i\omega T})\right\}. \end{aligned}$$

The employed multiplier can be transformed into the one for the small-gain theorem along the following lines:

$$\begin{aligned} 0 &\leq 2b \begin{pmatrix} \Delta(i\omega) \\ 1 \end{pmatrix}^* \begin{pmatrix} -2b & 1 \\ 1 & 0 \end{pmatrix} \begin{pmatrix} \Delta(i\omega) \\ 1 \end{pmatrix} \\ &= (\star)^* \left[\begin{pmatrix} 2b & -1 \\ 0 & 1 \end{pmatrix}^T \begin{pmatrix} -1 & 0 \\ 0 & 1 \end{pmatrix} \begin{pmatrix} 2b & -1 \\ 0 & 1 \end{pmatrix} \right] \begin{pmatrix} \Delta(i\omega) \\ 1 \end{pmatrix} \\ &= (\star)^* \begin{pmatrix} -1 & 0 \\ 0 & 1 \end{pmatrix} \begin{pmatrix} 2b\Delta(i\omega) - 1 \\ 1 \end{pmatrix} \\ &\iff |2b\Delta(i\omega) - 1| \leq 1. \end{aligned}$$

This links our arguments to those appearing in [**colgate2**, **colgate6**] and reveals that the direct application of tools from robust control allows to circumvent any transformation to scattering parameters (or, in other words, the application of a loop transformation) for obtaining the stability conditions. In fact, the congruence transformation

$$\left(\frac{1}{\sqrt{2b}}\begin{pmatrix}1 & -b\\ 1 & b\end{pmatrix}\right)^T \begin{pmatrix}-1 & 0\\ 0 & 1\end{pmatrix}\left(\frac{1}{\sqrt{2b}}\begin{pmatrix}1 & -b\\ 1 & b\end{pmatrix}\right) = \begin{pmatrix}0 & 1\\ 1 & 0\end{pmatrix}$$

with the scattering transformation matrix turns the small-gain multiplier into the one for passivity. This observation allows to easily show the equivalence of the small gain and passivity theorems through scattering transformations ([**andersonspong**]) and wave variable methods ([**nieslotine**, **nieslotine2**]).

§2.3.5 *Exactness of Robustness Tests*

As mentioned before, IQC-based stability criteria are typically only sufficient. Still the classical conditions as discussed in Sections **??**, **??** and **??** turn out to be also necessary. Necessity of these criteria can as well be seen to be a specialization of celebrated exactness results in structured singular-value theory. In fact, IQC robust stability tests for structured LTI uncertainties with two or three full diagonal blocks as derived above are known to be always exact. This implies, in particular, that our 3-port counterpart of Llewellyn's conditions is indeed a necessary and sufficient test for stability. It is far beyond the scope of this paper to provide all possible cases in which IQC-based robustness tests are known to be exact. For a detailed discussion related to LTI uncertainties we refer to [**packdoyle**, **fantits**, **cwssimax**].

We would like to emphasize that these beautiful exactness properties come at the price of some limitations of the classical framework. For instance, Llewellyn's conditions are not sufficient for stability any more if we only assume that the uncertainties are passive but not necessarily LTI. On the other hand, if allowing for arbitrary causal and passive uncertainties, stability is still guaranteed if we can find a frequency-independent $\lambda > 0$ which renders the FDI (**??**) satisfied, and this property can be easily verified numerically.

§2.4 BASIC IQC MULTIPLIER CLASSES

In the previous section, we have shown how classical frequency domain techniques can be embedded into the IQC formulation. In this section, we focus on the types of existing multipliers for different uncertainty classes. Although they frequently appear in the robust control literature, we include them for completeness.

§2.4.1 *Parametrized Passivity*

Another well-known version of the passivity theorem, which we will denote as theorem of parameterized passivity (see e.g. [**desvid**]), allows to consider cases in which the "non-passivity" of some block is compensated by an excess of passivity in other blocks without endangering stability. This can even be

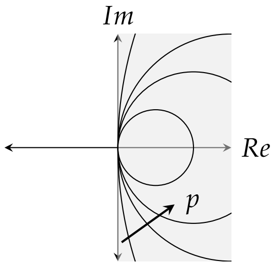

Figure 2.4: As p increases, the admissible region for the Nyquist curves of Δ shrinks to smaller disks in the right half plane.

utilized to determine the lowest tolerable level of passivity of the uncertainties for which a given interconnection remains stable. For output strictly passive uncertainties, stability can be characterized as in the next result, which is a direct consequence of the general IQC theorem.

Corollary 1. *Then interconnection of $G_p, \Delta \in \mathcal{RH}_\infty^{\bullet\times\bullet}$ as in Figure* **??** *is stable if there exist a $p \geq 0$ such that*

$$\begin{pmatrix} \Delta(i\omega) \\ I \end{pmatrix}^* \begin{pmatrix} -pI & I \\ I & 0 \end{pmatrix} \begin{pmatrix} \Delta(i\omega) \\ I \end{pmatrix} \succeq 0 \tag{2.25}$$

$$\begin{pmatrix} I \\ -G_p(i\omega) \end{pmatrix}^* \begin{pmatrix} -pI & I \\ I & 0 \end{pmatrix} \begin{pmatrix} I \\ -G_p(i\omega) \end{pmatrix} \prec 0 \tag{2.26}$$

hold for all $\omega \in \mathbb{R}_e$.

Remark 6. *Note that* (**??**) *and* (**??**) *are nothing but*

$$\Delta(i\omega) + \Delta^*(i\omega) \succeq p\,|\Delta(i\omega)|^2\,, \tag{2.27}$$

$$G_p(i\omega) + G_p^*(i\omega) \succ -pI. \tag{2.28}$$

The case $p = 0$ recovers the classical passivity theorem. Moreover, the larger the value of $p > 0$, the smaller is the set of uncertainties described by (**??**)*, as illustrated in Figure* **??** *for different values of p. In fact, this result is used in Colgate's condition thanks to the damping term b and closely related to the impedance bounds of Bounded Impedance Absolute Stability [***haddadizaad***] using "impedance circles".*

§2.4.2 *Real Parametric Uncertainties*

In many applications, the uncertainties originate from the lack of the precision on the actual values of the parameters in the system model. This applies in particular to the models used in bilateral teleoperation. Parameters such as the stiffness of the environment or the mass of the human arm are the simplest examples of this kind. The real parametric uncertainties are typically assumed to take values in some interval, say $[-r, r]$, centered around the nominal value zero; parameters in other intervals can be easily shifted in order to meet this requirement.

LTI uncertain parameters

The well-known DG multiplier family ([**meinsmafu**, **fantits**]) is used to assess robustness against unknown but constant parameters. In fact, for all bounded functions $D : \mathbb{R} \mapsto (0, \infty)$ and $G : \mathbb{R} \mapsto i\mathbb{R}$ one has

$$\begin{pmatrix} \delta \\ 1 \end{pmatrix}^* \begin{pmatrix} -D(\omega) & G(\omega) \\ G^*(\omega) & r^2 D(\omega) \end{pmatrix} \begin{pmatrix} \delta \\ 1 \end{pmatrix} \geq 0$$

for all $\delta \in [-r, r]$, just because it reads as

$$-D(\omega)|\delta|^2 + r^2 D(\omega) + (G(\omega)^* + G(\omega))\delta \geq 0;$$

this holds since $|\delta|^2 \leq r^2$, $D(\omega) \geq 0$ and $G(\omega) + G(\omega)^* = 0$.

Time-varying parameters with arbitrary rate of variation

In this case we employ constant multipliers; the time-varying parameter $\delta : [0, \infty) \mapsto [-r, r]$ satisfies the quadratic constraint

$$\begin{pmatrix} \delta(t) \\ 1 \end{pmatrix}^* \begin{pmatrix} -D & iG \\ -iG & r^2 D \end{pmatrix} \begin{pmatrix} \delta(t) \\ 1 \end{pmatrix} \geq 0$$

for all $D > 0$, $G \in \mathbb{R}$ and for all $t \geq 0$. This implies the validity of (**??**) for the multiplication operator which maps $v \in \mathcal{L}_2^n$ into $w \in \mathcal{L}_2^n$ with $w(t) = \delta(t)v(t)$.

Time-varying parameters with bounded rate of variation

If there is a known bound on the rate-of-variation (ROV) of the time-varying parameter, it is conservative to use constant DG scalings. To characterize slowly-varying real parametric uncertainties, we use the so-called "swapping lemma" ([**helmersson**, **jonsson**, **koroglu**], cf. [**packardteng**]) which allows to take the ROV bound explicitly into account. For the sake of completeness, we include a scalar version of this well known result from adaptive control.

Lemma 1 (Swapping Lemma). *Consider the bounded and differentiable function $\delta : [0, \infty) \to \mathbb{R}$ whose derivative is bounded as $|\dot{\delta}(t)| \leq d$ for all $t \geq 0$. Moreover, let $T(s) = C(sI - A)^{-1}B + D$ be a transfer function with a stable state-space realization and define*

$$T_c(s) := C(sI - A)^{-1}, \quad T_b(s) := (sI - A)^{-1}B.$$

If viewing T, T_c, T_b and δ (by point-wise multiplication) as operators $\mathcal{L}_2 \to \mathcal{L}_2$, one has $\delta T = T\delta + T_c\dot{\delta}T_b$ and thus

$$\underbrace{\begin{pmatrix} T & T_c \\ 0 & I \end{pmatrix}}_{T_{left}} \underbrace{\begin{pmatrix} \delta \\ \dot{\delta}T_b \end{pmatrix}}_{\Delta_s} = \underbrace{\begin{pmatrix} \delta & 0 \\ 0 & \dot{\delta}I \end{pmatrix}}_{\Delta_x} \underbrace{\begin{pmatrix} T \\ T_b \end{pmatrix}}_{T_{right}}$$

where x, s stand for "eXtended" and "Stacked" respectively.

We now claim that

$$\Pi(i\omega) = (\star)^* M_s \begin{pmatrix} T_{left}(i\omega) & 0 \\ 0 & T_{right}(i\omega) \end{pmatrix}$$

with

$$M_s = \begin{pmatrix} -D_a & 0 & iG_a & 0 \\ 0 & -D_b & 0 & iG_b \\ -iG_a & 0 & r^2 D_a & 0 \\ 0 & -iG_b & 0 & d^2 D_b \end{pmatrix}$$

for $T^* D_a T > 0$, $D_b > 0$ and $G_a, G_b \in \mathbb{R}$ is a valid IQC multiplier for the uncertainty Δ_s. In fact, one easily verifies

$$\begin{pmatrix} \Delta_x(t) \\ I \end{pmatrix}^T M_s \begin{pmatrix} \Delta_x(t) \\ I \end{pmatrix} \succeq 0 \;\text{ for all }\; t \geq 0$$

in the time domain. If we choose any $v \in \mathcal{L}_2$ and define

$$w = \begin{pmatrix} \Delta_x \\ I \end{pmatrix} T_{right} v,$$

we hence infer $\int_0^\infty w(t)^T M_s w(t)\, dt \geq 0$. On the other hand, due to Lemma **??**, we also have

$$w = \begin{pmatrix} T_{left}\Delta_s \\ T_{right} \end{pmatrix} v = \begin{pmatrix} T_{left} & 0 \\ 0 & T_{right} \end{pmatrix} \begin{pmatrix} \delta \\ \dot{\delta} T_b \\ 1 \end{pmatrix}$$

which proves the claim. Thus, after augmenting the corresponding channel with zero columns so as to make the plant compatible with Δ_s, the robustness test can be performed.

§2.4.3 *Delay Uncertainty*

The delay robustness problem has been studied extensively and the dominating approach is the use of scattering transformations/wave variable techniques, among other methods ([**leungfa**, **eusebi**, **andersonspong**, **nieslotine**, **nieslotine2**, **hokayemspong**, **yokokohji**, **lozano**, **arcara**, **parkcho**, **aziminejad**, **leespong**]). We refer to the survey article [**hokayemspong**] for a detailed exposition of these methods. A great deal of research has been devoted to delay robustness tests in robust control that are applicable to a wide class of teleoperation systems. We also refer to [**richard**] for a general treatment of the subject (e.g. based on Lyapunov-Krasovskii functionals) and to IQC based results as e.g. in [**scorletti**, **junsafonov**, **kaorantzer**, **niculescu**].

Here, we consider constant but uncertain delays and the maximum delay duration is bounded from above by $\bar{\tau} > 0$ seconds. We emphasize that it requires only a simple modification of the multiplier in order to arrive at robustness tests for different types of delays as reported in the literature.

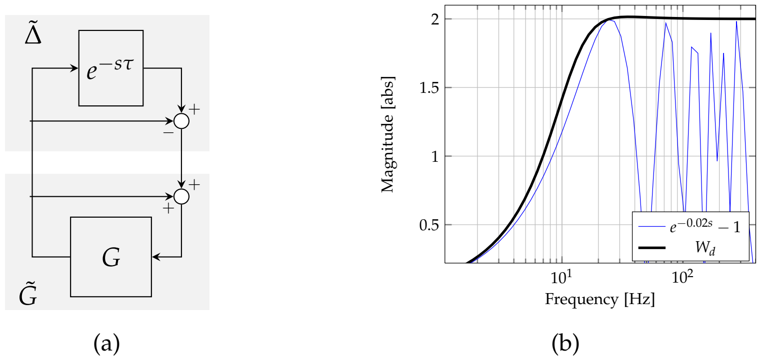

Figure 2.5: (a) Rewriting the delay LFT such that $\tau = 0$ implies $\tilde{\Delta} = 0$, (b)Frequency domain covering of the delay operator

If using the uncertainty $\Delta(s) = e^{-s\tau}$ in the configuration of Figure **??**, the nominal value $\tau = 0$ leads to $\Delta(s) = 1$ and not to zero as desired. This is resolved by rather employing the shifted uncertainty $\tilde{\Delta}(s) = e^{-s\tau} - 1$ and correspondingly modifying the system to $\tilde{G}$ (by unity feedback around G) as in Figure **??** and without modifying the interconnection.

The uncertainty is then characterized by using two properties of $\tilde{\Delta}$: For all ω, τ, the complex number $z = e^{-i\omega\tau} - 1$ is located on the unit circle centered at $(-1, 0)$ in the complex plane. Since condition $|z + 1| = 1$ translates into $z^*z + z^* + z = 0$, we infer for all bounded $\Omega : \mathbb{R} \to \mathbb{R}$ that

$$\begin{pmatrix} \tilde{\Delta}(i\omega) \\ 1 \end{pmatrix}^* \begin{pmatrix} \Omega(\omega) & \Omega(\omega) \\ \Omega(\omega) & 0 \end{pmatrix} \begin{pmatrix} \tilde{\Delta}(i\omega) \\ 1 \end{pmatrix} = 0 \ \ \forall \omega \in \mathbb{R} \tag{2.29}$$

for any delay time $\tau \in \mathbb{R}$. Furthermore, we need to take the low frequency property of the magnitude of the frequency response into account. This is typically captured by a frequency dependent weight. If we define,

$$W_d(s) = 2\frac{(s + \frac{4}{\pi\bar{\tau}})(s + \frac{\beta}{\bar{\tau}})}{(s - \frac{\pi}{2\bar{\tau}}e^{i\theta})(s - \frac{\pi}{2\bar{\tau}}e^{-i\theta})}$$

with $\theta = \left(\frac{\pi}{2}\right)^2$ and some small $\beta > 0$, then W_d covers the delay uncertainty in the sense that $|\tilde{\Delta}(i\omega)| \leq |W(i\omega)|$ for all $\omega \in \mathbb{R}$ and for all $\tau \in [0, \bar{\tau}]$. An example of magnitude covering is shown in Figure **??**.

This property, in turn, translates into $(\tilde{\Delta})^*\tilde{\Delta} \leq (W_d)^*W_d$ for all $\omega \in \mathbb{R}$. Then we can utilize the classical D-scalings to obtain the following constraint with a dynamic multiplier:

$$(\star)^* \begin{pmatrix} -\mathcal{D}(\omega) & 0 \\ 0 & W_d(i\omega)^*\mathcal{D}(\omega)W_d(i\omega) \end{pmatrix} \begin{pmatrix} \tilde{\Delta}(i\omega) \\ 1 \end{pmatrix} \geq 0 \tag{2.30}$$

for all bounded $\mathcal{D} : \mathbb{R} \to (0, \infty)$. Then the overall multiplier family results from a (conic) combination of those in (**??**) and (**??**):

$$(\star)^* \begin{pmatrix} -\mathcal{D}(\omega) + \Omega(\omega) & \Omega(\omega) \\ \Omega(\omega) & W_d(i\omega)^* \mathcal{D}(\omega) W_d(i\omega) \end{pmatrix} \begin{pmatrix} \tilde{\Delta}(i\omega) \\ 1 \end{pmatrix} \geq 0$$

for all $\omega \in \mathbb{R}$.

§2.5 Numerical Case Studies

In this section, we show how frequently encountered analysis problems can be solved under the IQC formulation with ease. We utilize the multipliers as given above for robustness tests applied to a simple teleoperation system taken from [**willaert**, **willaertIJRR10**]. Our main emphasis is on showing how one can reproduce the numerical results of such frequency domain techniques and, as the key contribution of this paper, how it is possible to substantially widen the range of allowed uncertainties in the IQC framework for which no classical analytical stability tests exist. This serves as an illustration for the possibility to improve analysis and, more importantly in future work, optimization-based controller synthesis results if better human/environment models become available.

§2.5.1 *Algorithmic Verification*

We have discussed some classical stability tests that reduce to explicit scalar inequalities which can be tested in a frequency-by-frequency fashion. In contrast, the equivalent re-formulations in terms of IQCs open the way to verifying these conditions numerically, by applying algorithms from the by now well-established area of semi-definite programming [**lmiboydbook**]. For example, checking at each frequency the existence of some diagonal $\Lambda \succ 0$ which satisfies (**??**) boils down to an efficiently tractable LMI problem in the three diagonal entries of Λ, which can be readily implemented in software environments such as [**yalmip**]. We also show how it is even possible to avoid any frequency-gridding and to reduce the tests to finite-dimensional semi-definite programming problems that can be solved in one shot.

This section serves to illustrate this procedure for Rollett's stability condition, which requires to determine a frequency-dependent bounded and strictly positive λ satisfying the FDI (**??**). Without loss of generality, it suffices to search for proper and rational functions λ that have no poles and are positive on the extended imaginary axis. Due to the well-established spectral factorization theorem (e.g. [**francis**]), we can express any such function as $\psi^*\psi$ with some stable transfer function ψ (without zeros in the closed right half-plane). For some fixed pole $a < 0$ let us choose the basis vectors

$$\Phi_n(s) = \begin{pmatrix} 1 & \frac{1}{s-a} & \frac{1}{(s-a)^2} & \cdots & \frac{1}{(s-a)^{n-1}} \end{pmatrix}^T$$

for $n = 0, 1, 2, \ldots$. By a well-known fact from approximation theory ([**pinkus**]), the function ψ can be approximated to an arbitrary degree by $L^T\Phi_n$ for some suitable $L \in \mathbb{R}^n$ uniformly on the imaginary axis, if only n is taken sufficiently large. More precisely, $\inf_{L\in\mathbb{R}^n} \|\psi - L^T\Phi_n\|_\infty$ converges to zero for $n \to \infty$. In summary, any proper rational λ with $\lambda(i\omega) > 0$ for $\omega \in \mathbb{R}_e$ can be approximated arbitrarily closely by $\Phi_n^* LL^T\Phi_n$ or, in turn, by

$$\Phi_n^* D\Phi_n \text{ with } D = D^T \in \mathbb{R}^{n\times n}.$$

This discussion justifies why one can parameterize the multiplier (middle term) in (**??**) as

$$\Psi_n^* \underbrace{\left(\begin{array}{cc|cc} -D & 0 & & \\ 0 & -1 & & \\ \hline & & D & 0 \\ & & 0 & 1 \end{array}\right)}_{M} \underbrace{\left(\begin{array}{cc|cc} \Phi_n & & & \\ & 1 & & \\ \hline & & \Phi_n & \\ & & & 1 \end{array}\right)}_{\Psi_n}$$

in terms of a frequency-dependent outer factor Ψ_n and a diagonally structured real symmetric matrix M in the middle. Let us denote the set of all these matrices M by $\mathcal{M}$ (where we drop the dependence on n). For checking Rollet's condition we then need to verify the existence of $M \in \mathcal{M}$ such that the FDIs

$$\Phi_n^* M\Phi_n \succ 0 \text{ and } \begin{pmatrix} I \\ S \end{pmatrix}^* \Psi_n^* M\Psi_n \begin{pmatrix} I \\ S \end{pmatrix} \prec 0$$

are satisfied. Let us finally introduce the minimal state space realizations

$$\Phi_n = \left[\begin{array}{c|c} A_\Phi & B_\Phi \\ \hline C_\Phi & D_\Phi \end{array}\right] \text{ and } \Psi_n \begin{pmatrix} I \\ S \end{pmatrix} = \left[\begin{array}{c|c} \mathcal{A} & \mathcal{B} \\ \hline \mathcal{C} & \mathcal{D} \end{array}\right].$$

This allows to apply the KYP Lemma in order to equivalently convert $\lambda > 0$ and (**??**) into the feasibility of the LMIs

$$\begin{pmatrix} I & 0 \\ A_\Phi & B_\Phi \\ C_\Phi & D_\Phi \end{pmatrix}^T \begin{pmatrix} 0 & Z & 0 \\ Z & 0 & 0 \\ 0 & 0 & D \end{pmatrix} \begin{pmatrix} I & 0 \\ A_\Phi & B_\Phi \\ C_\Phi & D_\Phi \end{pmatrix} \succ 0 \tag{2.31}$$

and

$$\begin{pmatrix} I & 0 \\ \mathcal{A} & \mathcal{B} \\ \mathcal{C} & \mathcal{D} \end{pmatrix}^T \begin{pmatrix} 0 & \mathcal{X} & 0 \\ \mathcal{X} & 0 & 0 \\ 0 & 0 & M \end{pmatrix} \begin{pmatrix} I & 0 \\ \mathcal{A} & \mathcal{B} \\ \mathcal{C} & \mathcal{D} \end{pmatrix} \prec 0. \tag{2.32}$$

More precisely, if one can computationally verify the existence of X, Z, $M \in \mathcal{M}$ and $D = D^T$ which satisfy (**??**) and (**??**), we have verified Rollet's condition. Conversely, if Rollet's condition holds, then these LMIs are guaranteed to have solutions if n is chosen sufficiently large.

Let us emphasize again that the very same procedure applies to considerable more complex interconnections and structured uncertainties Δ. In fact, for many interesting classes of uncertainties one can systematically construct multiplier families (see e.g. [**megretski**]) which are known to admit a description of the form

$$\Pi = \Psi^* M \Psi, \quad M \in \mathcal{M}$$

with a stable outer factor transfer matrix Ψ and with some set of structured symmetric matrices $\mathcal{M}$ that can itself be described as the feasible set of an LMI. Checking stability of the $G - \Delta$ interconnection in Figure **??** then requires to verify the validity of the FDI

$$\begin{pmatrix} I \\ G \end{pmatrix}^* \Psi^* M \Psi \begin{pmatrix} I \\ G \end{pmatrix} \prec 0.$$

Literally along the same lines as described above this is translated into a standard semi-definite program with the help of the KYP Lemma.

In what follows below, we will continue to utilize the shorthand notation of state-space realizations in a similar manner, i.e., $\mathcal{A}, \mathcal{B}, \mathcal{C}, \mathcal{D}$ for the combined outer factors by replacing S with the respective plant, and $A_\Phi, B_\Phi, C_\Phi, D_\Phi$ for the basis vector.

§2.5.2 *System Model*

In [**willaert**], a simple teleoperation system described with the following equations is considered:

$$\begin{aligned} F_h + \tau_m &= M_m \ddot{x}_m + B_m \dot{x}_m \\ \tau_s - F_e &= M_s \ddot{x}_s + B_s \dot{x}_s. \end{aligned}$$

Here M_m, M_s are the masses, B_m, B_s are the damping coefficients, τ_m, τ_s are the device motor torques, and x_m, x_s are the position coordinates of the local and the remote devices respectively (See the appendix for numerical data). F_h, F_e denote the human and the environment forces. The human and the environment are assumed to be LTI passive operators and are denoted by Δ_h, Δ_e which substitute Δ_s, Δ_l as employed in the more general network-related context in the earlier sections.

Additionally, a particular PD type of a position-force controller scheme, denoted by **P-F** , is used:

$$\tau_s = K_p(\mu x_m - x_s) - K_v \dot{x}_s, \quad \tau_m = -K_f F_e.$$

The overall teleoperation system is then described, with $Y_m(s) = \frac{1}{M_m s + B_m}$ and $Y_s(s) = \frac{\mu K_p}{M_s s^2 + (B_s + K_v)s + K_p}$, in terms of the following admittance matrix:

$$Y = \begin{pmatrix} Y_m & -K_f Y_m \\ -Y_m Y_s & \frac{M_m s^2 + B_m s + \mu K_f K_p}{(M_s s^2 + (B_s + K_v)s + K_p)} Y_m \end{pmatrix}. \tag{2.33}$$

As shown in [**willaert**], the system's performance is related to the transparency of the teleoperator, which is characterized by the maximal attainable product μK_f while maintaining stability. Therefore, we will evaluate our results with respect to this performance measure.

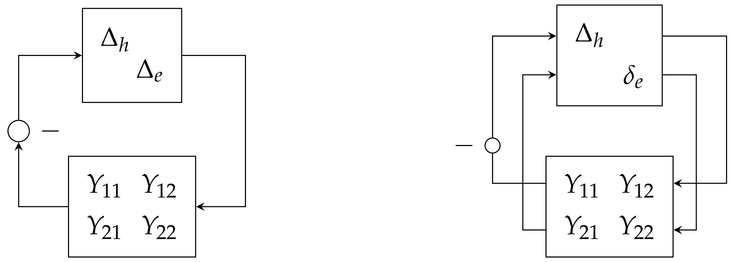

(a) Unconditional stability (b) Uncertain stiff environment

Figure 2.6: System interconnections for Section **??** and Section **??**.

§2.5.3 *Case 1 : Unconditional Stability Analysis via IQCs*

We start with applying Llewellyn's test based on (**??**) to the system given above. In a first computation, we choose a frequency grid of 2000 logarithmically spaced points in $[0, 10000]\,\frac{\text{rad}}{\text{s}}$ and solve, at each grid point, a feasibility problem in $\lambda > 0$. This is incorporated into a bisection algorithm that searches for the maximum value of μK_f for which feasibility at each grid-point can be guaranteed. Due to gridding, this method typically gives an upper bound rather than the exact value on the guaranteed performance level, just because the is a chance to miss critical frequencies. Nevertheless, we have obtained the exact value ≈ 0.137 as in [**willaert**]. The inner search for λ requires 8.52 s, while the overall computation takes about 117 s; note that the latter heavily depends on the initial bisection interval and on the desired accuracy.

In a second computation, we follow the path as described in Section **??**. The resulting FDI is

$$\left(\Psi\begin{pmatrix} I \\ -Y \end{pmatrix}\right)^* M \left(\Psi\begin{pmatrix} I \\ -Y \end{pmatrix}\right) \prec 0 \tag{2.34}$$

where

$$\Psi = \left(\begin{array}{cc|cc} \Phi & 0 & 0 & 0 \\ 0 & 1 & 0 & 0 \\ \hline 0 & 0 & \Phi & 0 \\ 0 & 0 & 0 & 1 \end{array}\right), \quad M = \left(\begin{array}{cc|cc} 0 & 0 & M_1 & 0 \\ 0 & 0 & 0 & 1 \\ \hline M_1 & 0 & 0 & 0 \\ 0 & 1 & 0 & 0 \end{array}\right) \tag{2.35}$$

with some unstructured real symmetric matrix M_1.

All this leads to the following stability test.

Corollary 2. *The $Y - \Delta$ interconnection depicted in Figure* **??** *is stable for all passive blocks Δ_h and Δ_e if there exist symmetric matrices $\mathcal{X}, Z, M_1$ with*

$$\begin{pmatrix} I & 0 \\ \mathcal{A} & \mathcal{B} \\ \mathcal{C} & \mathcal{D} \end{pmatrix}^T \begin{pmatrix} 0 & \mathcal{X} & 0 \\ \mathcal{X} & 0 & 0 \\ 0 & 0 & M \end{pmatrix} \begin{pmatrix} I & 0 \\ \mathcal{A} & \mathcal{B} \\ \mathcal{C} & \mathcal{D} \end{pmatrix} \prec 0$$

and

$$\begin{pmatrix} I & 0 \\ A_\Phi & B_\Phi \\ C_\Phi & D_\Phi \end{pmatrix}^T \begin{pmatrix} 0 & Z & 0 \\ Z & 0 & 0 \\ 0 & 0 & M_1 \end{pmatrix} \begin{pmatrix} I & 0 \\ A_\Phi & B_\Phi \\ C_\Phi & D_\Phi \end{pmatrix} \succ 0.$$

We applied Corollary **??** with a basis of length $n = 8$ and with the pole $a = -7$. In this way we computed again the maximal value $\mu K_f \approx 0.137$ for which stability can be guaranteed in about 36 s.

Remark 7. *Since Y is strictly proper,* (**??**) *cannot be satisfied at $\omega = \infty$ because its left-hand side vanishes. However, the interconnection is certainly well-posed such that the FDI only needs to be verified for all finite frequencies (Remark **??**). Therefore, the gridding approach can be applied directly. In the alternative path without gridding, we can circumvent this trouble by replacing Y with $Y + \epsilon I$, with $\epsilon = 10^{-5}$ in our case. Let us stress that this perturbation (also in the cases presented below) is only required in those channels that are related to passive uncertainties.*

§2.5.4 *Case 2: Unconditional Stability with Uncertain Stiff Environments*

We characterize the admissible environments as pure springs modeled by $Z_e = \frac{k}{s}$ with an uncertain constant stiffness coefficient $k \in [0, \bar{k}]\ \frac{\mathrm{N}}{\mathrm{m}}$. After merging $-\frac{\bar{k}}{s}$ with the system (and slightly perturbing the pole of the integrator to render the nominal system stable) we are left with the uncertainty structure $\Delta = \mathrm{diag}(\Delta_h, \delta_e)$ where the human uncertainty is assumed to be passive LTI and δ_e is an uncertain real scalar parameter in the interval $[0, 1]$. Using a modified DG-scaling for the shifted parameter range, we can easily adapt the multiplier and obtain, next to $\lambda > 0$ and $d > 0$, the following FDI for interconnection stability:

$$(\star)^* \left(\begin{array}{cc|cc} 0 & 0 & \lambda & 0 \\ 0 & -d & 0 & \frac{d}{2} + ig \\ \hline \lambda & 0 & 0 & 0 \\ 0 & \frac{d}{2} - ig & 0 & 0 \end{array}\right) \left(\begin{array}{cc} 1 & 0 \\ 0 & 1 \\ \hline -Y_{11} & -Y_{12} \\ Y_{21} & Y_{22} \end{array}\right) \prec 0. \qquad (2.36)$$

With the frequency grid as in the previous case we obtained too optimistic results (after comparing the values with those computed below), which suggests the need to refine the frequency grid. With additional 1500 points in the interval $[10^{-6}, 100]\,\frac{\mathrm{rad}}{\mathrm{s}}$, we obtained the exact value of $(\mu K_f)_{\max} \approx 0.215$ for $\bar{k} = 1000\frac{\mathrm{N}}{\mathrm{m}}$ in 127.7 s. We infer that the grid resolution, whether logarithmic or linear, plays a crucial role for the computations.

This reveals that, especially for systems that have high bandwidth and complex dynamics, it is instrumental to choose a sufficiently fine frequency grid in stability analysis. This is the very reason for the alternative path of computations (via multiplier parametrization and LMIs in state-space) as proposed above. In this particular example, the resulting condition boils down to two simple LMIs to be verified numerically. After normalizing the environment uncertainty by scaling, we just need to verify feasibility of the LMIs in the next result.

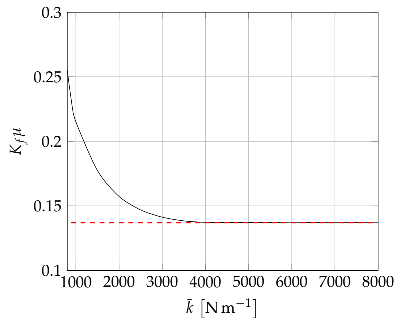

Figure 2.7: Performance loss for increasing environment stiffness uncertainty. The dashed line shows the value for unconditional stability from Section **??**

.

Corollary 3. *The $Y - \Delta$ interconnection in Figure* **??** *is stable for all passive LTI Δ_h and LTI real parametric uncertainty $\delta_e \in [0, 1]$ if there exist symmetric matrices $\mathcal{X}, Z_2, D_2$ and a skew symmetric matrix G_2 such that*

$$\begin{pmatrix} I & 0 \\ \mathcal{A} & \mathcal{B} \\ \mathcal{C} & \mathcal{D} \end{pmatrix}^T \begin{pmatrix} 0 & \mathcal{X} & 0 \\ \mathcal{X} & 0 & 0 \\ 0 & 0 & M \end{pmatrix} \begin{pmatrix} I & 0 \\ \mathcal{A} & \mathcal{B} \\ \mathcal{C} & \mathcal{D} \end{pmatrix} \prec 0$$

and

$$\begin{pmatrix} I & 0 \\ A_\Phi & B_\Phi \\ C_\Phi & D_\Phi \end{pmatrix}^T \begin{pmatrix} 0 & Z_2 & 0 \\ Z_2 & 0 & 0 \\ 0 & 0 & D_2 \end{pmatrix} \begin{pmatrix} I & 0 \\ A_\Phi & B_\Phi \\ C_\Phi & D_\Phi \end{pmatrix} \succ 0$$

hold, where

$$M = \left(\begin{array}{cc|cc} 0 & 0 & 1 & 0 \\ 0 & -D_2 & 0 & \frac{1}{2}D_2 + G_2 \\ \hline 1 & 0 & 0 & 0 \\ 0 & \frac{1}{2}D_2 - G_2 & 0 & 0 \end{array}\right), \Psi = \left(\begin{array}{cc|cc} 1 & 0 & 0 & 0 \\ 0 & \Phi_2 & 0 & 0 \\ \hline 0 & 0 & 1 & 0 \\ 0 & 0 & 0 & \Phi_2 \end{array}\right).$$

For this example we have used the basis Φ_2 with length 12 and selected the pole location as $a = -16$. Bisection over μK_f took 29.3 s and the resulting maximum admissible value is found to be 0.215 for a sample value of $\bar{k} = 1000$. Values higher than 0.215 would render the nominal system unstable, which means that we obtain the best possible result. The performance curve for different values of $\bar{k}$ is given in Figure **??**.

§2.5.5 *Case 3: Robustness against Delays*

We reconsider the plant given in (**??**) and modify it in order to relate the results to the undelayed cases given above. We assume that there exist communication delays present in the forward and backward path and, without loss of generality, we choose both maximally allowed delay durations to be equal for simplicity. We thus consider

$$Y = \begin{pmatrix} Y_m & -K_f Y_m e^{-s\tau} \\ -Y_m Y_s \mu K_p e^{-s\tau} & \frac{M_m s^2 + B_m s + \mu K_f K_p e^{-2s\tau}}{(M_s s^2 + (B_s + K_v)s + K_p)(M_m s + B_m)} \end{pmatrix}$$

where $\tau \in [0, \bar{\tau}]$. By pulling out the delay uncertainties from Y, the nominal plant Y_d is given by

$$Y_d = \begin{pmatrix} Y_m & 0 & -Y_m & 0 \\ 0 & sY_s & 0 & -K_p Y_s \\ 0 & K_f & 0 & 0 \\ \mu Y_m & 0 & -\mu Y_m & 0 \end{pmatrix}$$

and is interconnected to the structured uncertainty block

$$\Delta = \operatorname{diag}\left(\Delta_h, \Delta_e, e^{-s\tau}, e^{-s\tau}\right).$$

By following the procedure given in Section **??**, a unity feedback is applied and two delay weights are included in the plant.

Corollary 4. *The $Y_d - \Delta$ interconnection is stable for all passive LTI Δ_h, Δ_e and LTI delay uncertainties if there exist symmetric matrices $\mathcal{X}, M_1, M_2, D_3, D_4, R_3, R_4$ and Z_i for $i = 1, \dots, 4$ such that*

$$\begin{pmatrix} I & 0 \\ \mathcal{A} & \mathcal{B} \\ \mathcal{C} & \mathcal{D} \end{pmatrix}^T \begin{pmatrix} 0 & \mathcal{X} & 0 \\ \mathcal{X} & 0 & 0 \\ 0 & 0 & P \end{pmatrix} \begin{pmatrix} I & 0 \\ \mathcal{A} & \mathcal{B} \\ \mathcal{C} & \mathcal{D} \end{pmatrix} \prec 0$$

and

$$\begin{pmatrix} I & 0 \\ A_\Phi^i & B_\Phi^i \\ C_\Phi^i & D_\Phi^i \end{pmatrix}^T \begin{pmatrix} 0 & Z_i & 0 \\ Z_i & 0 & 0 \\ 0 & 0 & \Upsilon_i \end{pmatrix} \begin{pmatrix} I & 0 \\ A_\Phi^i & B_\Phi^i \\ C_\Phi^i & D_\Phi^i \end{pmatrix} \succ 0$$

hold for $i = 1, \dots, 4$, where $\Upsilon_1 = M_1$, $\Upsilon_2 = M_2$, $\Upsilon_3 = D_3$, $\Upsilon_4 = D_4$,

$$\begin{aligned} P &= \begin{pmatrix} P_{11} & P_{12} \\ P_{12}^T & P_{22} \end{pmatrix} \\ P_{11} &= \operatorname{diag}\left(0, 0, -D_3, R_3, -D_4, R_4\right), \\ P_{12} &= \operatorname{diag}\left(M_1, M_2, 0, R_3, 0, R_4\right), \\ P_{22} &= \operatorname{diag}\left(0, 0, D_3, 0, D_4, 0\right). \end{aligned}$$

and

$$\Psi = \left(\begin{array}{cccc|cccc}
\Phi_1 & & & & & & & \\
& \Phi_2 & & & & & & \\
& & \Phi_3 & & & & & \\
& & \Phi_5 & & & & & \\
& & & \Phi_4 & & & & \\
& & & \Phi_6 & & & & \\
\hline
& & & & \Phi_1 & & & \\
& & & & & \Phi_2 & & \\
& & & & & & \Phi_3 W_d & \\
& & & & & & \Phi_5 & \\
& & & & & & & \Phi_4 W_d \\
& & & & & & & \Phi_6
\end{array}\right).$$

This test is applied for various maximum delay durations $\bar{\tau} \in [0.01, 0.1]$s with 0.005s increments and the results are shown in Figure **??**. At each $\bar{\tau}$ point, the bisection algorithm took on average 577.4s (varying in $[435, 1040]$s). The basis lengths and the pole locations are selected as $n_i = 3, 3, 3, 3, 5, 5$ and $a_i = -16, -17, -19, -8, -13, -14$ respectively. The pole locations are selected away from the system's poles but arbitrary otherwise.

§2.5.6 *Additional Remarks*

In concluding this section, we would like to address the issue of conservatism in our numerical examples. The first two cases involve none at all for sufficiently long basis functions as confirmed numerically.

If considering only passive LTI uncertainties in standard problems, there is no room for further algorithmic improvements since the resulting tests are guaranteed to be exact. On the other hand, there is a huge potential in searching for refined uncertainty characterizations in order to reduce conservatism. We have illustrated that there is no need to confine the analysis to passive uncertainties as long as they can be associated with some integral quadratic constraint, possibly through some physical experiments. Thus, once IQCs are known for individual uncertainty blocks, it has been also demonstrated how to computationally verify robust stability against their combined influence on the interconnection with ease.

On the other hand, this might not be the case for the test in Corollary **??**. To quantify the potential conservatism, we use extreme values for the stiff environment and the delay uncertainty and determine the maximum achievable values of μK_f for which the transfer function seen by the human is still strictly passive. Environments that are modeled as pure stiffnesses are considered to be "worst cases" since their Nyquist curves are located at the boundary of the closed right half plane and since their low frequency contribution, unlike pure mass models, is significant. As shown in Figure **??**, the performance decreases for increasing levels of $\bar{\tau}$ and $\bar{k}$, but the trade-off curve does not change significantly beyond the value $\bar{k} = 100\,000\,\mathrm{N\,m^{-1}}$. We have also overlayed the

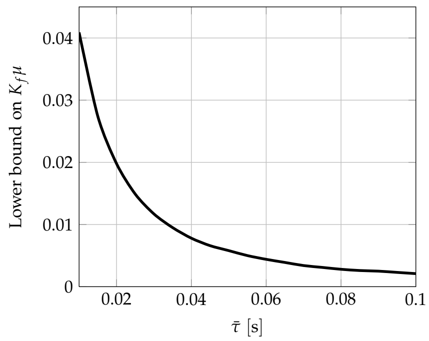

Figure 2.8: Performance loss for increasing maximal delay duration.

results of Figure **??**. If it is indeed true that a pure stiffness environment is the worst case, then the difference between the two lowest curves in Figure **??** can be attributed to the conservatism of the test in Corollary **??**. Remarkably, we have actually quantified the conservatism and can conclude that it is not very large; this is of particular significance for delay-independent robust stability tests which would result in values in the range of $\mu K_f \approx 10^{-5}$.

Let us briefly compare with results obtained for time-varying environments. This makes a particularly interesting case since, in practice, a remote device might explore environments with varying characteristics. We have analyzed the non-delayed system where the environment is a pure spring with a stiffness coefficient $k(t) \in [0, 1000]\mathrm{N\,m}^{-1}$ and different bounds on the rate-of-variation as shown in Figure **??**. Classical absolute stability tests can only handle arbitrary fast variations which leads to small values of performance of $\approx 2 \cdot 10^{-5}$. The inclusion of information about the ROV (as possible through the class of multipliers discussed above) substantially reduces the conservatism as is visible in the plot.

We include a final remark about the performance criterion. In the literature, one often encounters PID-based controller architectures which makes it possible to analyze the effect of variations in the controller gains onto the performance of the teleoperation system. In our set-up, we can attribute the increase of performance to the increase of μK_f due to the simplicity of the system structure. If moving towards more complicated controller architectures, such clear relations are not expected to be valid any more. This precludes obtaining graphical or analytical stability and performance tests with robustness guarantees. Although not made explicit for reasons of space, the IQC framework allows the incorporation of a performance channel and to develop robust performance analysis tests, very much along the same lines as discussed for stability in this paper.

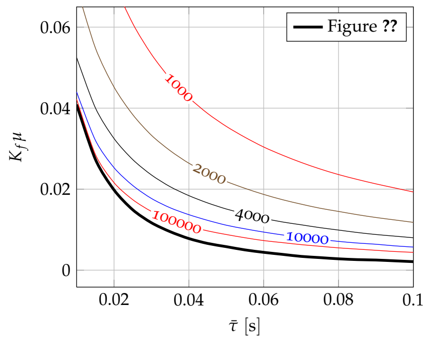

Figure 2.9: Robust performance for different stiff environment cases in the face of increasing delay uncertainty duration

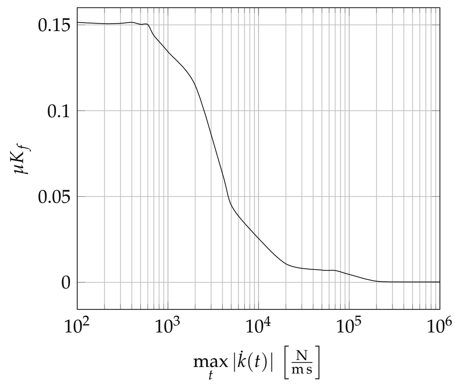

Figure 2.10: The performance loss with respect to the increase in ROV bound of the time-varying uncertaint parameter $k(t) \in [0, 1000]\,\mathrm{N\,m^{-1}}$.

§2.6 CONCLUSIONS

In this paper, we advocate the application of the IQC framework to achieve refined analysis results and to highlight the need for models tailored for bilateral teleoperation. For this purpose, we have provided a number of theoretical and numerical analysis examples, all of which are special cases of the IQC theorem. We emphasize the link between contemporary and celebrated classical analysis results in the literature and reveal how to obtain substantial generalizations. Our examples show that the quality of the characterization of uncertainties is the key for improved analysis results.

We strongly believe that the proposed framework together with task dependent human and environment models would lead to substantial improvements for both stability analysis and model-based controller synthesis.

CHAPTER 3

Synthesis

The synthesis problem that we want attack requires a human model together with the local/remote devices. We will delay the environment discussion until the next section. Our framework can be shown pictorially in Figure **??**. Here we assume that the human is watching a screen that

We start with the identified model [**fucavus**] : The basic block diagram is given in Figure **??**. The signal relations can be written as

$$\begin{pmatrix} q \\ x \end{pmatrix} = \begin{bmatrix} 0 & W_{unc} \\ H_{arm} & H_{arm} \end{bmatrix} \begin{pmatrix} p \\ f \end{pmatrix}$$

For our purposes we obtain a mapping from position to force via a partial inversion on the second channel.

$$\begin{pmatrix} q \\ f \end{pmatrix} = \begin{bmatrix} -W_{unc} & W_{unc} H_{arm}^{-1} \\ -1 & H_{arm}^{-1} \end{bmatrix} \begin{pmatrix} p \\ x \end{pmatrix} = \begin{bmatrix} W_{unc} \\ 1 \end{bmatrix} \begin{bmatrix} -1 & H_{arm}^{-1} \end{bmatrix} \begin{pmatrix} p \\ x \end{pmatrix}$$

The LTI transfer function H is strictly proper hence its inverse is non-proper. Since we are only interested in the frequency response up to 200 Hz we use a low-pass filter on the position to tame the high frequency behavior.

$$W_t = \frac{4000}{s^2 + 280s + 40000}$$

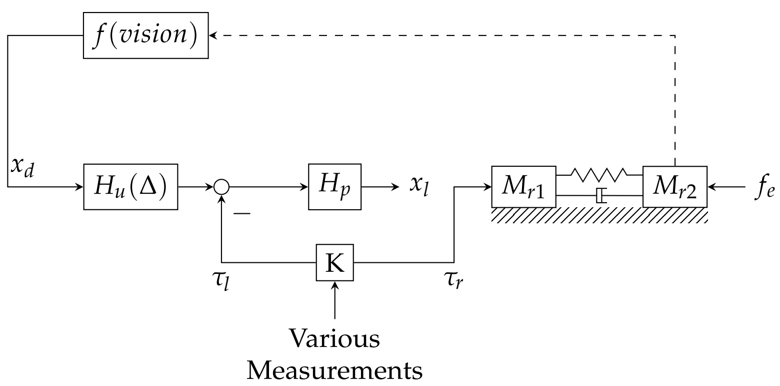

Figure 3.1: The general framework

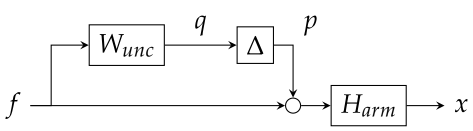

Figure 3.2: The experimentally identified human model from [**fucavus**]

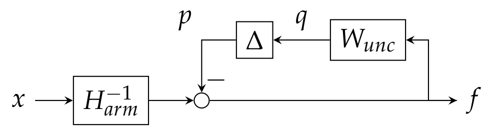

Figure 3.3: The mapping is inverted to obtain a model from position to force.

After the application of this filter we obtain the overall human operator as

$$\begin{pmatrix} q \\ f \end{pmatrix} = \begin{bmatrix} W_{unc} \\ 1 \end{bmatrix} \begin{bmatrix} -1 & H_{arm}^{-1} W_t \end{bmatrix} \begin{pmatrix} p \\ x \end{pmatrix} = H_u \begin{pmatrix} p \\ x \end{pmatrix}$$

The next step is the obtain a local device model from force to position. We have selected the commercial PHANTOM device model which is identified in [**cavusfeygintendick**]. The model is given by the following transfer function:

$$H_p = \frac{1}{s^2} \frac{s^2 + 5.716s + 9.201 \cdot 10^4}{(3.329 \cdot 10^{-6} s^2 + 0.001226s + 1.536)}$$